ISSN (Print): 2476-8316
ISSN (Online): 2635-3490
Dutse Journal of Pure and Applied Sciences (DUJOPAS), *Vol. 7 No. 1 March 2021*

Structural, Elastic and Electronic Properties of an Orthorhombic Carbon Allotrope: A first-principles calculation

Ibrahim Buba Garba[1,2], Abdullahi Lawal[3], Idris Muhammad Chiromawa[4]

[1]Department of Physics,
Federal University Gashua,
PMB 1005, Gashua,
Yobe State, Nigeria.

[2]Institut de Minéralogie,
de Physique des Matériaux et de Cosmochimie (IMPMC),
Sorbonne Université
4 place Jussieu, 75005
Paris, France.

[3]Department of Physics,
Federal College of Education Zaria,
P.M.B, 1041, Zaria,
Kaduna State, Nigeria.

[4]Department of Physics,
Sule Lamido University Kafin-Hausa,
Jigawa State, Nigeria

Abstract
In this paper, structural, elastic, lattice dynamics, electronic and thermal properties of a new orthorhombic allotrope of carbon (C16) is systematically investigated using first-principles calculations within generalized gradient approximation (GGA) and local density approximation (LDA). We found the ground state structural parameters to be in agreement with recent theoretical results. Analysis of the elastic constants and phonon dispersion spectra reveals that the structure is mechanically and dynamically stable at ambient pressure. Band structure calculations show that C16 has indirect bandgap of value 3.12eV, making it suitable for high-power electronics applications. The large bulk modulus of 390Gpa andVicker's hardness of 81 GPa indicate that the structure is superhard. The origin of its hardness can be attributed to stiffer sp3 bonds between the carbon atoms which gives a smaller Poisson ratio, and a large Debye temperature.

Keywords: C16, DFT, Thermal properties, Debye temperature, Vicker's hardness.

INTRODUCTION
Advances in high-pressure experimental techniques and theoretical methods have led to the discovery of several materials with interesting properties for various scientific and industrial

**Author for Correspondence*

applications. Carbon has the ability to form various structures either by forming sp-, sp2- and sp3- coordination(Miller et al., 1997), which give rise to a wide range of behavior such as insulating, semiconducting, superconducting, metallic, and even recently magnetic properties(Fang et al., 2020). Compressed graphite transforms to diamond (Irifune et al., 2003, Sumiya and Irifune, 2007)above15GPa at a higher temperature. The graphite-diamond transition can be achieved by applying pressure and heat using either laser-driven static compression(Irifune et al., 2003)or dynamic explosive shocks(Kraus et al., 2016). Recently, nanodiamonds have also been synthesized by irradiating graphite with ultraviolet photons(de Castro et al., 2021). At low temperatures, experimental and theoretical studies suggested that compressed graphite transforms to new allotropes of carbon including W-carbon (Wang et al., 2011), T-Carbon(Wang et al., 2011, Xu et al., 2020), and M-carbon(Bu et al., 2019). An orthorhombic carbon with Pbcm symmetry was also proposed by Bu et al(Bu et al., 2019) and the simulated x-ray diffraction (XRD) spectra match that of diamond-rich coatings from the experiment(Choudhary et al., 2017). The proposed material is a wide bandgap semiconductor, which was shown to be superhard, and stable at ambient pressure based on analysis of elastic, dynamic, and thermal properties. For fundamental understanding and practical application, deeper insight into the physical propertiesof a material is necessary.

Using first-principles density functional theory,we first establish the structural, elastic, and dynamic stability of the orthorhombic carbon (C16) with the Pbcn space group symmetry. Then we systematically study the electronic and mechanical properties, including Vicker's hardness, elastic anisotropy, speed of sound, and the Debye temperature. Importantly, we observed that C16 is a superhard, anisotropic, and wide bandgap material, with Vicker's hardness comparable to that diamond.

COMPUTATIONAL METHOD

Density functional theory (DFT) as implemented in Quantum Espresso package(Giannozzi et al., 2009, Giannozzi et al., 2017) is used to make a theoretical prediction on C16. The Perdew-Burke_Ernzerh (PBE) (Perdew et al., 1996) scheme of the generalized gradient approximation (GGA) and Perdew-Zunger(PZ) (Perdew and Zunger, 1981) local density approximation (LDA) were adopted for the exchange-correlation functional. Core and valence electrons interaction was treated using Ultrasoft pseudopotentials(Vanderbilt, 1990) obtained from QE Pslibrary(Baroni et al., 2001) . The electronic wave-functions are expanded using a plane-wave basis with a kinetic energy cutoff of 50Ry. Brillouin zone is sampled with Monkhorst-Pack grid of 8x8x8 k-points and the convergence parameters of energy and force were set to be 10-5Ry and 10-4Ry/au, respectively. The two symmetry in inequivalent Wyckoff sites for this orthorhombic carbon structure. These two sites are 8d (0.17333, -0.08534, 0.02354) and 8d(0.16635, 0.62965, 0.21215)Density functional perturbation theory (DFPT) (Baroni et al., 2001) was used to calculate phonon dispersion along the high symmetry path in the Brillouin zone using $4 \times 4 \times 4$q-rid. Thermo_pw(Dal Corso, 2016)code was employed to compute elastic properties using the stress-strain method. Ions were relaxed for each deformation, and the stiffness matrix Cij corresponding to nine independent elastic constants was obtained for the orthorhombic structure (Laue class D_2h (mmm))

RESULTS AND DISCUSSIONS

Structural Properties and Stability

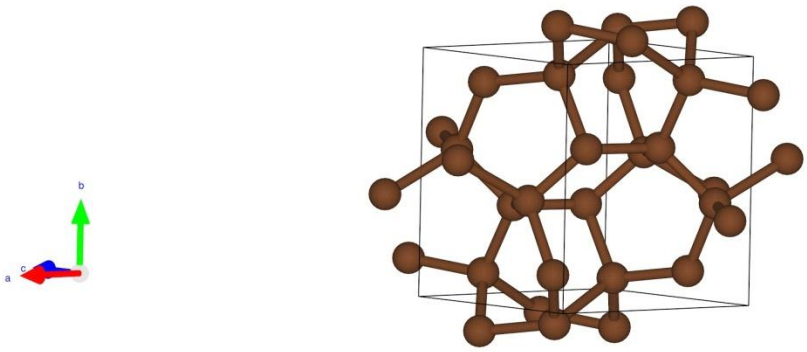

Figure 1: The crystal structure of C16 in an orthorhombic unit cell containing 16 atoms with sp3 bonded coordination.

Figure 1 shows C16, which belongs to the space group Pbcn (No. 60) with 16 atoms per orthorhombic unit cell. The two Wyckoff sites occupied by C atoms are 8d(0.15943 -0.08580 0.01187) and 8d(0.16739 0.63196 0.20359). GGA and LDA optimized lattice parameters for C16 are presented in Table 1, along with that of diamond for comparison. Subsequent calculations of electronic band structure, phonon dispersion, and elastic properties are performed using the GGA optimized lattice parameters. For the diamond structure, the lattice constants are in excellent agreement with the experimental result of Occelli et al. (Occelli et al., 2003) which attests to the validity of the method adopted in predicting properties of the new carbon allotrope. As can be observed from Table 1, LDA underestimates the lattice parameter of diamond and overestimate bulk modulus, while GGA functional has the opposite effect i.e. overestimate the lattice parameter and underestimate the bulk modulus.

To assess the stability of crystal material, it is pertinent to examine its mechanical, dynamic, and thermodynamic properties. The mechanical stability of the predicted structures will be discussed in the subsequent section. The dynamic stability of the structure is examined by computing the phonon dispersion spectra. The absence of negative frequency throughout the Brillouin zone indicates that the structure is dynamically stable at zero pressure (Figure 2). Furthermore, the highest vibrational frequency of C16 at the gamma point is $523cm^{-1}$, which is comparable to that of diamond $517cm^{-1}$, and slightly less than that of conjugated graphite (Maultzsch et al., 2004). However, while diamond have 2 atoms per unit cell and six phonon branches (3 acoustic and 3 optical modes), C16 have 16 atoms in its orthorhombic unit cell which gives 48 phonon branches (3 acoustic and 45 optical modes)

Table 1. Calculated lattice parameters a, b and c, volume per atom, V, Bulk modulus, B, and its derivative B′, for C16 and comparison to the cubic diamond. Superscripts represent results from the literature.

Structure	Space group	Method	a(A)	b(A)	c(A)	V(A³/Atom)	B(GPa)	B′
C16	Pbcm	LDA	4.386	4.720	4.366	5.65	420	3.88
		GGA	4.437	4.771	4.405	5.83	385	4.03
C-16	Pbcm	GGA[a]	4.438	4.771	4.407	5.83	422	
Diamond	Fd-3m	LDA	3.536			5.53	454	3.78
		GGA	3.571			5.69	419	3.84
		EXP[b]	3.567			5.67	442	3.01

a: ref (Bu et al., 2019)
b: ref (Occelli et al., 2003)

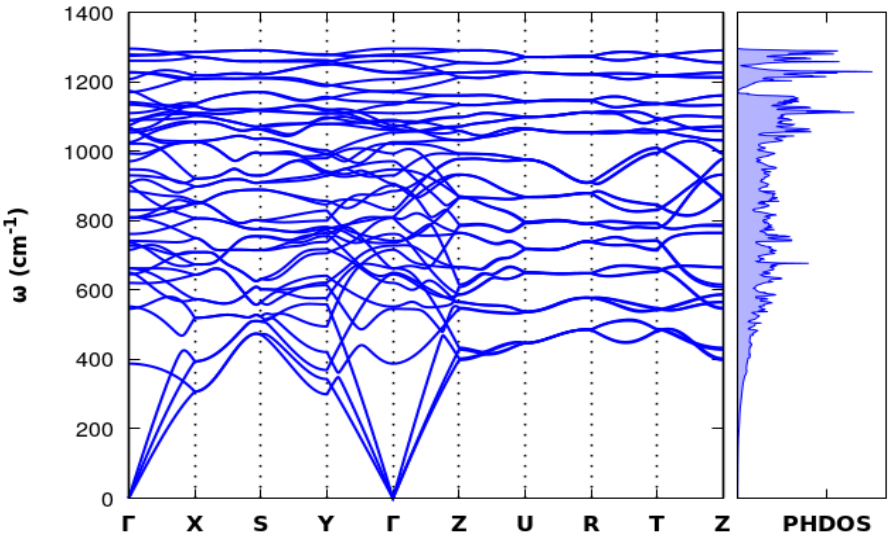

Figure 2: The phonon dispersion spectra and density of states of C16 along the high symmetry direction in the Brillouin zone. There are no soft (negative) frequencies and therefore the structure is dynamically stable at ambient pressure.

Elastic properties

The calculated elastic constants Cij (Gpa) of C16 using VRH approximationand that of the diamond, with comparison to experiment and other theoretical work are presented in Table 2. The Elastic constants of material provide insight into important properties such as stiffness, mechanical stability, bonding character, ductility, brittleness, and anisotropic character. Neglecting zero-point energy, the stiffness matrix,C_{ijkl}, is defined as the derivative of the stress, σ, with respect to strain,ε_{ij} which is also related to the second derivative of the DFT total energy of the structure, E with respect to the strains ε_{ij}:

$$C_{ijkl} = \left(\frac{\partial \sigma_{ij}}{\partial \varepsilon_{jkl}}\right) = \left(\frac{\partial^2 E}{\partial \varepsilon_{ij} \partial \varepsilon_{jk}}\right) \quad (1)$$

For an orthorhombic crystal, there are nine independent elastic constants that must satisfy the Born-Huang stability criteria (Fan et al., 2014):

$$C_{ii} > 0;\ i = 1,2..6,$$

$$[C_{11} + C_{22} + C_{33} + 2(C_{12} + C_{13} + C_{23})] > 0,$$
$$(C_{11} + C_{22} - 2C_{12}) > 0,$$
$$(C_{11} + C_{33} - 2C_{12}) > 0,$$
$$(C_{22} + C_{33} - 2C_{23}) > 0.$$

Apparently, from the values of the computed C_{ij} in Table 2, these conditions are fully satisfied, and therefore the material is mechanically stable. Furthermore, the higher value ofC_{33} indicates that the structure is more incompressible along the c-axis than either x-, or y-axis. The bulk modulus B, shear modulus, G, Young's modulus E, and Poisson's ratio are also computed using Voigt-Reuss-Hill approximation (Hill, 1952) and the result is presented in Table 3. Pugh (Pugh, 1954) proposed that material is said to be ductile if the ratio of its bulk to shear modulus, B/G, is greater than 1.75, otherwise, it manifests a brittle feature. Poisson ratio can also give insight into the brittle and ductile nature of materials. Materials with v greater than 0.26 are ductile, and when v is less than 0.26, then they behave as brittle. Clearly, C16 is brittle since the B/G ratio is 0.867 and the Poisson ratio is 0.08.

Table 2. The calculated elastic constants Cij (Gpa) of C16 using VRH approximation[23] and that of the diamond, with comparison to experiment and other theoretical work.

Pressure (GPa)	Method	C_{11}	C_{12}	C_{13}	C_{22}	C_{23}	C_{33}	C_{44}	C_{55}	C_{66}
Diamond	This work	1120	154					608		
	LDA[c]	1107	149					594		
	EXP[d]	1076	125					577		
C16-Wang	GGA	962	93	123	1013	129	1182	528	554	340
C16	GGA	916	78	82	961	104	1124	496	525	339

c: ref (Grimsditch and Ramdas, 1975)
d: ref (Niu et al., 2014)

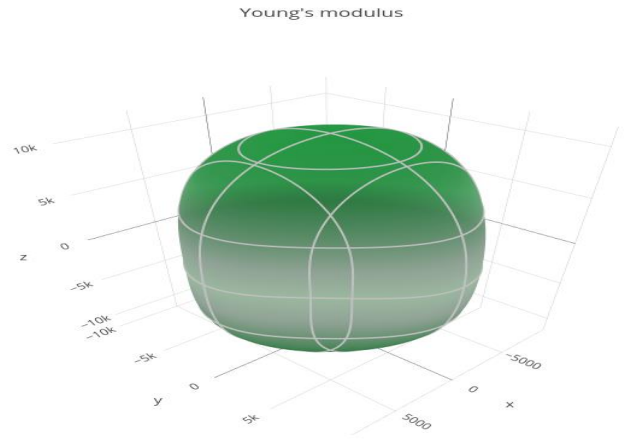

Figure 3: A 3D directional dependence of Young's modulus for orthorhombic C16 phase.

To understand the anisotropic property of the structure, we compute the universal anisotropic index A^U, given by

$$A^U = 5(G_V/G_R) + B_V/B_R - 6 \quad (2)$$

whereB_V and G_V are the bulk and shear modulus from Voigt approximation while B_R and G_R are bulk and shear modulus from Reuss approximation, respectively. Evidently, C16 deviates from the isotropic character, with the universal isotropic index, $A^U = 0.295$. A three-dimensional surface construction of Young's modulus directional dependence of C16 is shown in Figure 3. A spherical shape always indicates isotropic structure which implies that physical properties do not change with crystallographic directions. Any deviation from a spherical shape implies that a structure is anisotropic. Accordingly, the orthorhombic C16 structure is anisotropic.

The hardness of a material is another quantitative way of expressing its elastic or plastic behavior. There are different models used in estimating the hardness of a material and here we adopted Chen's model(Chen et al., 2011)since it gives results much closer to the experiment. According to this model, the hardness of a material,H_V is given by

$$H_V = 2.0(G^3/B^2)^{0.585} - 3.0 \quad (3)$$

The hardness of diamond using this model and experimental elastic moduli is 95 GPa, which is in excellent agreement with experimental measurement (Occelli et al., 2003). The predicted hardness of C16 is 81 GPa, closer to that of the diamond, and materials with hardness greater than 40GPa are classified as superhard materials.

Table 3. Calculated elastic moduli, Poisson's ratio v, and Hardness for C16, in comparison with experimental and theoretical results for diamond.

Structure	Method	B(GPa)	G(GPa)	B/G(GPa)	v	H_v
Diamond	LDA[e]	468	545	0.858	0.08	92
	EXPT[f]	442	534	0.827	0.07	95
C16-wang						
C16	GGA	390	450	0.867	0.08	81

e: (Niu et al., 2014)
f: (Grimsditch and Ramdas, 1975)

Thermal Properties

The Debye temperature is a fundamental property of solid material and can be used to understand the nature of interatomic bonding and also estimate melting temperature. A larger Debye temperature indicates stronger bonds and higher melting temperature. Using results from electronic structure calculation and the elastic moduli, the Debye temperature can be obtained from Eq 4:

$$\Theta_D = \frac{h}{k_B} v_m \left[\frac{3n}{\pi}\left(\frac{N_A\rho}{M}\right)\right]^{1/3} \quad (4)$$

$$v_m = \left[\frac{1}{3}\left(\frac{2}{v_G^3} + \frac{1}{v_P^3}\right)\right]^{-1/3} \quad (5)$$

$$v_P = \sqrt{\left(B + \frac{4}{3}G\right)\frac{1}{\rho}} \quad (6)$$

$$v_G = \sqrt{\frac{G}{\rho}} \quad (7)$$

$$v_B = \sqrt{\frac{B}{\rho}} \quad (8)$$

wherev_P, v_G, v_B and v_m, are the compressional, shear, bulk, and average sound velocities, respectively. h, k_B, and N_A are the Planck's, Boltzmann's,and Avogadro's constants, respectively, n is the number of atoms per unit cell, M is the molecular weight, and ρ is the density of crystal. The Debye temperature, sound velocities, and density of the crystal are presented in Table 4. The melting temperature of a solid can also be estimated from its bulk modulus using T= 607 + 9.3B +- 555

Table 4. Mass density (ρ in$g.cm^{-3}$) compressional, bulk, shear, average elastic sound velocities (v p , v s , v m in m/s) and the estimated Debye temperature (Θ_D in K).

Structure	ρ(g.cm^{-3})	v_P(m.s^{-1})	v_B(m.s^{-1})	v_G(m.s^{-1})	v_m(m.s^{-1})	Θ_D(K)
Diamond	3.628	18308	11460	12364	13474	2273
C16	3.533	16736	10517	11274	12271	2030

Electronic properties

The electronic properties of a material determine its suitability for various applications, including optoelectronics, photovoltaics, and high power electronics. The electronic band structure and density of states are calculated and presented in Figure 4. The valence band maximum (VBM) is located at the gamma point, while the conduction band maximum is at the S point of the orthorhombic Brillouin zone, indicating that the C16 is an indirect bandgap semiconductor. Close to the gamma point, the bang is dispersed, which indicates better carrier mobility. The bandgap value is 3.8 eV, but the tendency of DFT to underestimate the bandgap of materials is well known, and therefore experimental band gap should be expected to be higher. The total density of states and the contribution of the different orbital from C1 and C2 are also presented. Evidently, the p orbitals of C1 and C2 give the most contribution close to the Fermi level compared to their 2s counterparts.

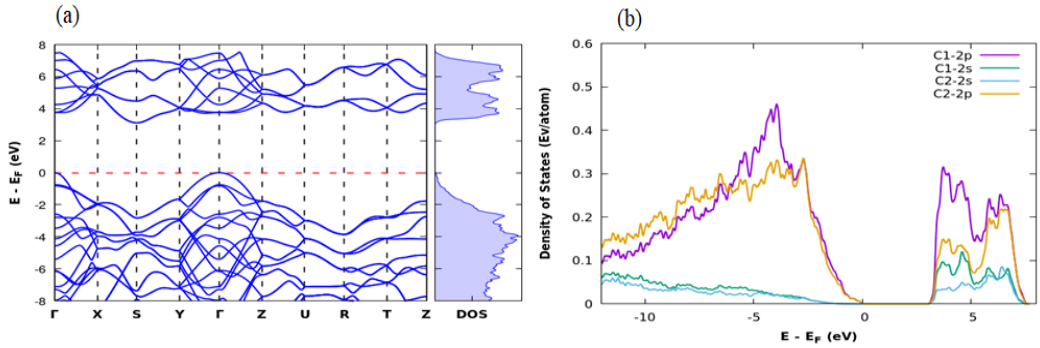

Figure 3: (a) Electronic band structure and density of states of C16 (b) Partial density of states of C16, indicating large contribution from C1 and C2 p orbitals

CONCLUSION

In summary, we perform first-principles calculations to investigate the structural, elastic, lattice dynamics, electronic as well as thermal properties of a new orthorhombic allotrope of carbon with Pbcn symmetry. We found the ground state structural parameters to be in agreement with recent theoretical results. Analysis of the elastic constants and phonon dispersion spectra reveals that the structure is mechanically and dynamically stable at ambient pressure. Band structure calculations show that it is a semiconductor with an indirect bandgap of 3.12eV, making it suitable for high-power electronics applications. The large bulk modulus (390GPa) and Vicker's hardness 81 GPa indicate that the structure is superhard. The origin of its hardness can be attributed to stiffer sp3 bonds between carbon atoms which gives a smaller Poisson ratio, and a large Debye temperature.

REFERENCE

Baroni, S., De Gironcoli, S., Dal Corso, A. & Giannozzi, P. 2001. Phonons and related crystal properties from density-functional perturbation theory. *Reviews of modern Physics,* 73**,** 515.

Bu, K., Wang, J.-T., Li, Z.-Z., Mizuseki, H. & Kawazoe, Y. 2019. A superhard orthorhombic carbon with all six-membered-ring in sp3 bonding networks. *Physics Letters A,* 383**,** 2809-2812.

Chen, X.-Q., Niu, H., Li, D. & Li, Y. 2011. Modeling hardness of polycrystalline materials and bulk metallic glasses. *Intermetallics,* 19**,** 1275-1281.

Choudhary, R., Mishra, S., Mishra, P., Limaye, P. & Sastry, P. 2017. Mechanical and tribological properties of rhombohedral diamond-rich coatings grown on stainless steel by hot filament CVD. *Transactions of the IMF,* 95**,** 197-202.

Dal Corso, A. 2016. Elastic constants of beryllium: a first-principles investigation. *Journal of Physics: Condensed Matter,* 28**,** 075401.

De Castro, A. I. G., Rheinstädter, M., Clancy, P., Castilla, M., De Isidro, F., Larruquert, J. I., De Lis-Sánchez, T., Britten, J., Piris, M. C. & De Isidro-Gómez, F. P. 2021. Graphite to diamond transition induced by photoelectric absorption of ultraviolet photons. *Scientific Reports,* 11**,** 1-7.

Fan, Q., Wei, Q., Yan, H., Zhang, M., Zhang, D. & Zhang, J. 2014. A New Potential Superhard Phase of OsN 2. *Acta Physica Polonica, A.,* 126.

Fang, H., Masaki, M., Puthirath, A. B., Moya, J. M., Gao, G., Morosan, E., Ajayan, P. M., Therrien, J. & Jena, P. 2020. U-carbon: metallic and magnetic. *arXiv preprint arXiv:2008.01137*.

Giannozzi, P., Andreussi, O., Brumme, T., Bunau, O., Nardelli, M. B., Calandra, M., Car, R., Cavazzoni, C., Ceresoli, D. & Cococcioni, M. 2017. Advanced capabilities for materials modelling with Quantum ESPRESSO. *Journal of Physics: Condensed Matter,* 29**,** 465901.

Giannozzi, P., Baroni, S., Bonini, N., Calandra, M., Car, R., Cavazzoni, C., Ceresoli, D., Chiarotti, G. L., Cococcioni, M. & Dabo, I. 2009. Quantum Espresso: a modular and open-source software project for quantum simulations of materials. *Journal of physics: Condensed matter,* 21**,** 395502.

Grimsditch, M. & Ramdas, A. 1975. Brillouin scattering in diamond. *Physical Review B,* 11**,** 3139.

Hill, R. 1952. The elastic behaviour of a crystalline aggregate. *Proceedings of the Physical Society. Section A,* 65**,** 349.

Irifune, T., Kurio, A., Sakamoto, S., Inoue, T. & Sumiya, H. 2003. Ultrahard polycrystalline diamond from graphite. *Nature,* 421**,** 599-600.

Kraus, D., Ravasio, A., Gauthier, M., Gericke, D., Vorberger, J., Frydrych, S., Helfrich, J., Fletcher, L., Schaumann, G. & Nagler, B. 2016. Nanosecond formation of diamond and lonsdaleite by shock compression of graphite. *Nature communications,* 7**,** 1-6.

Maultzsch, J., Reich, S., Thomsen, C., Requardt, H. & Ordejón, P. 2004. Phonon dispersion in graphite. *Physical review letters,* 92**,** 075501.

Miller, E., Nesting, D. C. & Badding, J. 1997. Quenchable transparent phase of carbon. *Chemistry of materials,* 9**,** 18-22.

Niu, C.-Y., Wang, X.-Q. & Wang, J.-T. 2014. K 6 carbon: A metallic carbon allotrope in sp 3 bonding networks. *The Journal of chemical physics,* 140**,** 054514.

Occelli, F., Loubeyre, P. & Letoullec, R. 2003. Properties of diamond under hydrostatic pressures up to 140 GPa. *Nature materials,* 2**,** 151-154.

Perdew, J. P., Burke, K. & Ernzerhof, M. 1996. Generalized gradient approximation made simple. *Physical review letters,* 77**,** 3865.

Perdew, J. P. & Zunger, A. 1981. Self-interaction correction to density-functional approximations for many-electron systems. *Physical Review B,* 23**,** 5048.

Pugh, S. 1954. XCII. Relations between the elastic moduli and the plastic properties of polycrystalline pure metals. *The London, Edinburgh, and Dublin Philosophical Magazine and Journal of Science,* 45**,** 823-843.

Sumiya, H. & Irifune, T. 2007. Hardness and deformation microstructures of nano-polycrystalline diamonds synthesized from various carbons under high pressure and high temperature. *Journal of materials research,* 22**,** 2345-2351.

Vanderbilt, D. 1990. Soft self-consistent pseudopotentials in a generalized eigenvalue formalism. *Physical review B,* 41**,** 7892.

Wang, J.-T., Chen, C. & Kawazoe, Y. 2011. Low-temperature phase transformation from graphite to s p 3 orthorhombic carbon. *Physical review letters,* 106**,** 075501.

Xu, K., Liu, H., Shi, Y.-C., You, J.-Y., Ma, X.-Y., Cui, H.-J., Yan, Q.-B., Chen, G.-C. & Su, G. 2020. Preparation of T-carbon by plasma enhanced chemical vapor deposition. *Carbon,* 157**,** 270-276.